ISSN 0010-9525, Cosmic Research, 2016, Vol. 54, No. 2, pp. 118–126. © Pleiades Publishing, Ltd., 2016.
Original Russian Text © A.V. Gerasimov, D.B. Dobritsa, S.V. Pashkov, Yu.F. Khristenko, 2016, published in Kosmicheskie Issledovaniya, 2016, Vol. 54, No. 2, pp. 126–134.

Theoretical and Experimental Study of a Method for the Protection of Spacecraft from High–Speed Particles

A. V. Gerasimov[a], D. B. Dobritsa[b], S. V. Pashkov[a], and Yu. F. Khristenko[a]

[a] *Tomsk State University, Tomsk, 634050 Russia*

[b] *Lavochkin Research and Production Association, Khimki, Moscow oblast, 141400 Russia*

e-mail: ger@mail.tomsknet.ru

Received April 15, 2014

Abstract—In this paper, we perform numerical simulation and experimental determination of the limiting resistance of the spacecraft design elements used when developing anti-meteorite protection of spacecraft as well as protection against space debris. One possible way to increase the efficiency of protective shields and satisfy the requirements of the mass characteristics of the latter is the use of mesh barriers.

DOI: 10.1134/S0010952516020015

1. INTRODUCTION

The problem of the reliable protection of manned and unmanned spacecraft for the study of near-earth and deep space has become very important at present, due to the increasing duration of the flights of these objects, increasing the probability of collision of the latter with space bodies or technogeneous fragments, occurring as a result of the destruction of orbital constructions. The collision of fragments with bodies and other elements of spacecraft can lead to penetration or destruction, malfunctions, and even more serious consequences for manned objects.

In 1947 [1], Whipple proposed a method of protecting spacecraft from the impact of high-speed cosmic particles by placing a thin shield in front of the spacecraft body for fragmenting and redistributing the momentum of striking fragments over most of the area of the protected body, where it interacts with a thin shield. This allows for the provision of the necessary degree of protection within a given range of masses and collision velocities of particles for the established mass-dimensional parameters of the spacecraft. It should be noted that the problem of the reduction of the mass of the protective spacecraft elements, while maintaining efficiency, remains actual.

It follows from a review of the literature that the process of high-speed interaction of solid shields with strikers has been studied quite fully, and the process of the interaction of a striker with mesh shield is still insufficiently studied.

Experiments on the high-speed introduction of a polyethylene striker (striker dimension is 15 mm) to a string shield (the string material is steel, the string diameter is 0.5–1.0 mm) were carried out in [2]. The goal is the experimental proof of a qualitative difference between the nature of striker destruction, when it interacts with a string shield, and destruction for a solid shield. Impact velocity varied in the range of 1.7–3.0 km/s. Polyethylene has a lower (in comparison with aluminum striker) resistance to introduction; therefore, effects specific to the introduction of a discrete shield in the striker, according to the authors, should appear more clearly.

The results of a set of experiments in which the ability of various shields to influence the degree of striker fragmentation was evaluated, are presented in [3]. A protective design consisting of aluminum meshes and a solid shield separated by a small distance was found to be the most effective. As shown by the authors [4], a combination of a mesh and a solid shield allows us to reduce the mass of the protective system by approximately 30–40% in comparison with the Whipple scheme. In [5], the authors presented the results of a wide study of the nature of high-speed fragmentation of strikers on discrete and continuous barriers clarifying the features of interaction of both single meshes and a sequence of meshes with strikers. A set of experiments for fragmenting aluminum strikers on steel meshes [6] showed the dependence of the form of striker fragmentation on the geometric parameters of meshes.

In [7], the authors present the results of 12 experiments for evaluating the resistance of shield protection from high-speed penetration at velocities of 2.66–3.44 km/s. It is known that this range of velocities is most dangerous for shield protection and corresponds to the minimum ballistic dependence of the critical size of the aluminum striker on the impact velocity. As a striker, an aluminum ball (the AD-1 alloy) is used, with a diameter of 6.35 mm and mass of 0.39 g.

Schemes of protective designs includes two or more mesh shields consisting of one or more steel meshes with different geometric and mass characteristics. The works presented above operate with sufficiently large particles as strikers, but of great practical interest are particles with a diameter of 2 mm or less, operating in a range of 2.66–3.44 km/s, the problem of the protection from which is presently resolved, taking into account computational capabilities and modern materials.

To simulate the collisions of high-speed particles with samples of protection, light-gas guns were mainly used, allowing us to accelerate the strikers (with the dimensions mentioned in the papers) up to space velocities. For particles with a diameter of 2 mm or less, with the diameter of light-gas gun barrels of large calibers, it is necessary to use methods allowing us to throw strikers with significantly less dimensions from these facilities.

Without neglecting the importance of experimental studies it should also be noted that performing mass tests in a wide range of dimensions and velocities of strikers, materials, thicknesses and designs of protective shields requires large material and financial costs. The application to the study of this problem of modern computers and numerical methods allowing us to solve the problems of high-speed collision in a three-dimensional statement taking into account the fragmentation of strikers and protective elements of the spacecraft design seems an actual and practically important problem. The numerical simulation of high-speed interaction of solids allows us to reproduce at acceptable costs the characteristic features of physical processes occurring in collision and to consider and choose optimal protection schemes.

The natural heterogeneity of the structure of the plate material and technogeneous fragments influencing the distribution of physical and mechanical characteristics (FMC) of the material is a main factor determining the nature of the destruction of real materials. Accounting for this factor in the equations of mechanics of deformable solid bodies is possible using the random distribution of the initial deviations of the strength properties from nominal values (the simulation of the initial defective structure of material).

The ratios of the mechanics of deformable solid bodies used in modern works on the dynamic destruction of designs and materials does not take into account that this factor can distort the real picture of the impact destruction of the considered bodies. This becomes particularly apparent in solving axisymmetric problems, where all points on circular coordinates of the calculated element are initially equivalent in view of the standard equations of continuum mechanics used in numerical simulation. In practice, however, there is a wide range of problems where fragmentation is mostly a probabilistic process, for example, the explosive destruction of axisymmetric shells where the nature of fragmentation is not known beforehand, the penetration and destruction of thin barriers by a striker along normal to the surface, etc. Adding the random distribution of the initial deviations of the strength properties from the nominal value in the FMC body leads to the fact that, in these cases, the process of destruction takes on a probabilistic character more consistent with experimental data.

It should be noted that in [2, 6, 7] the results of calculations using the SPH method, which satisfactorily transmits a qualitative picture of the process of collision of a particle and a mesh, has a low accuracy in quantifying collision parameters.

2. BASIC RATIOS

Equations describing the motion of a compressible elastic–plastic body taking into account the probabilistic nature of destruction. Equations describing the spatial adiabatic motion of a solid compressible medium are differential consequences of the fundamental laws of conservation of mass, momentum, and energy. In general, they have the following form [8, 9]:

equation of continuity

$$\frac{1}{\rho}\frac{d\rho}{dt} + \frac{\partial v_i}{\partial x_i} = 0; \tag{1}$$

equation of motion

$$\rho\frac{dv_i}{dt} = \rho F_i - \frac{\partial P}{\partial x_i} + \frac{\partial S_{ij}}{\partial x_j}; \tag{2}$$

equation of energy

$$\rho\frac{dE}{dt} = S_{ij}\varepsilon_{ij} + \frac{P}{\rho}\frac{d\rho}{dt}, \tag{3}$$

where x_i are coordinates; t is time; ρ_0 is the initial density of the medium; ρ is the current density of the medium; v_i are the components of the velocity vector; F_i are the components of the vector of mass forces; S_{ij} are the components of the stress tensor deviator; E is the specific internal energy; ε_{ij} are the components of the deviator of deformation velocity tensor; and P is pressure.

To Eqs. (1)–(3) it is necessary to add equations taking into account the corresponding thermodynamic effects connected with the adiabatic compression of the medium and the strength of the medium. In the general case, when the forces act on a solid deformable body, change occurs both in the volume (density) and the shape of the body, in this case, according to various dependences. Therefore, the stress tensor is represented as the sum of the spherical tensor and the stress tensor deviator

$$\sigma_{ij} = S_{ij} - P\delta_{ij}, \quad i, j = 1, 2, 3,$$
$$\delta_{ij} = 1, \quad i = j, \ \delta_{ij} = 0, \quad i \neq j,$$

where δ_{ij} the Kronecker symbol.

To describe the shift resistance of the body, we use the following ratios:

$$2\mu\left(e_{ij} - \frac{1}{3}e_{kk}\delta_{ij}\right) = \frac{DS_{ij}}{Dt} + \lambda S_{ij}; \quad (4)$$

$$\frac{DS_{ij}}{Dt} = \frac{dS_{ij}}{dt} - S_{ik}\omega_{jk} - S_{jk}\omega_{ik}; \quad (5)$$

$$2\omega_{ij} = \frac{\partial v_i}{\partial x_j} - \frac{\partial v_j}{\partial x_i}; \quad (6)$$

$$2e_{ij} = \frac{\partial v_i}{\partial x_j} + \frac{\partial v_j}{\partial x_i}, \quad (7)$$

as well as the condition of plasticity

$$J_2 = \frac{1}{2}S_{ij}S_{ij} = \frac{1}{3}\sigma^2, \quad (8)$$

where e_{ij} are components of the deformation velocity tensor; μ is the rigidity modulus; σ is the dynamic yield strength; and D/Dt is Yauman's derivative.

The equation of the rigid body state was chosen in the Mie–Gruneisen form

$$P = \frac{K(1 - \Gamma_0\xi/2)}{(1 - c\xi)^2}\xi + \rho_0\Gamma_0 E, \quad (9)$$

where Γ_0 is the Gruneisen coefficient; c, K are constants of the material; ρ_0 is the initial density of the medium; and $\xi = 1 - \rho_0/\rho$.

Moreover, we take into account that, in high-speed interactions, two mechanisms of destruction can be implemented: shifting and slabbing. As a criterion for shifting destruction, a criterion of limiting equivalent plastic deformation was used [10], namely $\varepsilon^p = \varepsilon^p_*$. In this case, when ε^p reaches the limiting value ε^p_*, the calculated cell is considered to be destroyed. The system of equations (1)–(9) was written in a general form for the dimensional motion of a deformable body.

In real materials, the process of destruction is always determined by the internal structure of the medium, the presence of inhomogeneities, as a rule, caused by different orientations of grains in the polycrystalline material or inhomogeneities in the composition of composite materials, the difference in microstrengths inside a grain, and the intergranular or interphase boundary. Therefore, to increase the adequacy of the numerically simulated process it is necessary for experimental data to introduce disturbances in the physical and mechanical characteristics of the destroyed medium, i.e., random distribution of the factors determining the strength properties of the material. Introducing into the calculation method information on the polycrystalline structure of the material requires a large amount of experimental data and increased requirements of computer engineering power, limiting the ability of the implementation and application of this approach. In this connection, in this paper, we use a simplified version of the simulation of the probabilistic mechanism of destruction. The physical and mechanical characteristics of the medium ξ_i responsible for the strength are considered to be distributed randomly over the material volume. The probability density of the distribution of the given parameters $dp/d\xi_i = f_i(\xi_i, \xi_{0i}, D_i, \Omega_j)$ is taken as the different laws of the distribution f_i, generally depending on the table (average) value ξ_{0i} of the distributed parameter of variable dispersion D_i of the distribution of this parameter, and other characteristics of the medium Ω_j. For gradientless single-phase material, characteristics such as density, rigidity modulus, and modulus of volume compression are practically independent of the number of defects and, when distributed over a volume, these values can be considered constant. At the same time, parameters such as yield strength, ultimate strength, maximum deformation, and other constants determining the time of occurrence of destruction in various theories of strength and destruction criteria directly depend on the number and dimensions of defects and should be distributed randomly over the volume, with dispersion depending on material homogeneity. The natural fragmentation of the thick-walled elastic–plastic shell and barrier is calculated by introducing a probabilistic mechanism of the distribution of the initial defects of the material structure to describe the slabbing and shifting cracks. As a criterion of the destruction at intensive shifting deformations, the achievement of equivalent plastic deformation of its limiting value is used in the problems. Initial inhomogeneities were simulated by the fact that the limiting equivalent plastic deformation was distributed in shell cells with a modified random number generator, creating a random value submitting to the chosen distribution law. The probability densities of random values were taken as a normal Gaussian distribution, with an arithmetic mean equal to the table value and variable dispersion.

The system of the basic equations is complemented by the necessary initial and boundary conditions. At the initial time, all points of the striker have axial velocity V_0 in view of their sign, and the barrier state is supposed to be undisturbed. The boundary conditions are set as follows: on boundaries free from stress, the following conditions are met: $\sigma_n = \tau_n = 0$. On the area of contact between the bodies the condition is put of ideal sliding of one material relative to another along the tangent, as well as the condition of nonflowing along the normal: $\sigma_{n1} = \sigma_{n2}$, $v_{n1} = v_{n2}$, $\tau_{n1} = \tau_{n2} = 0$, where σ_n, τ_n are normal and tangential components of the stress vector; v_n is normal component of the velocity vector at the point of contact; and indices 1 and 2 refer to the contact bodies.

Experimental results

Test number	Throwing facility	Striker	Tested barrier and shield	Velocity of collision, km/s	Experimental result
F5	MPKH 23/8 with cutter	Duralumin ball with 2-mm diameter	Tank + 0.32-mm mesh + 0.2-mm mesh	2.1	Through mesh penetration. Tracks with depth of 0.3–0.5 mm from fragments on tank
F7	MPKH 23/8	Duralumin ball with 2-mm diameter	Tank + 0.32-mm mesh + 0.2-mm mesh	2.1	Through mesh penetration. Tracks with depth of 0.3–0.5 mm from fragments on tank
F8	MPKH 23/8 with cutter	Duralumin ball with 2-mm diameter	Tank + 0.32-mm mesh + 0.2-mm mesh	2.1	Through mesh penetration. Tracks with depth of 0.3–0.5 mm from fragments on tank
F16	MPKH 23/8 with cutter	Duralumin ball with 2-mm diameter	Tank + 0.32-mm mesh + 0.2-mm mesh	4.0	Through mesh penetration. Tracks with depth of ~0.5 mm from fragments on tank
F17	MPKH 23/8 with cutter	Duralumin ball with 3.3-mm diameter	Tank + 0.32-mm mesh + 0.2-mm mesh	4.0	Through mesh penetration. No visible damages on tank
F18	MPKH 23/8 with cutter	Duralumin ball with 1-mm diameter	Tank + 0.32-mm mesh + 0.2-mm mesh	4.0	Through first mesh penetration. No visible damages on the second mesh and tank
F23	MPKH 23/8 with cutter	Duralumin ball with 2-mm diameter	Tank + 0.32-mm mesh + 0.2-mm mesh	2.9	Through mesh penetration. No visible damages on tank
F26	MPKH 23/8 with cutter	Duralumin ball with 3-mm diameter	Tank + equivalent shield of 1-mm duralumin	2.9	Through penetration of shield and tank
F27	MPKH 23/8 with cutter	Duralumin ball with 3-mm diameter	Tank + 0.32-mm mesh + 0.2-mm mesh	2.9	Through mesh penetration. Convexity on tank at backside and tracks from fragments of ~1 mm
F29	MPKH 23/8 with cutter	Duralumin ball with 2-mm diameter	Tank + 0.32-mm mesh = EVTI	2.9	Through penetration of mesh and EVTI. Convexity on tank at backside and tracks from fragments of ~1 mm

To calculate the elastic–plastic flows, a method is used that is implemented on tetrahedral cells and based on the combined use of the Wilkins method for calculating interior points of the body and the Johnson method for calculating contact interactions [8, 11–13]. Partitioning the three-dimensional area into tetrahedrons occurs sequentially by means of subprograms for automatic meshing. The most complete ideology and methodology of the probabilistic approach to the problem of destruction of solids are shown in [14].

3. TEST CALCULATIONS

The problem of the expansion of a copper shell with a steel ring on it under the action of detonation products was considered [14].

The calculated mesh used in this calculation was approximately 500000 tetrahedral cells. To describe the destruction, a method of splitting over nodes was used: when performing the destruction criterion in the vicinity of the node, splitting nodes and the formation of the destruction surface occur. To simulate the initial irregularities, the distribution of the limiting value of equivalent plastic deformation over the cells of the calculated area was used according to the normal law with a dispersion of 10% deviation.

With the expansion of the ring, a localization of deformations was observed in the vertices of the radial cracks formed in the initial inhomogeneities and the formation of sufficiently large fragments. The calculated fragmentation spectrum agrees quite satisfactorily with experimental data [15].

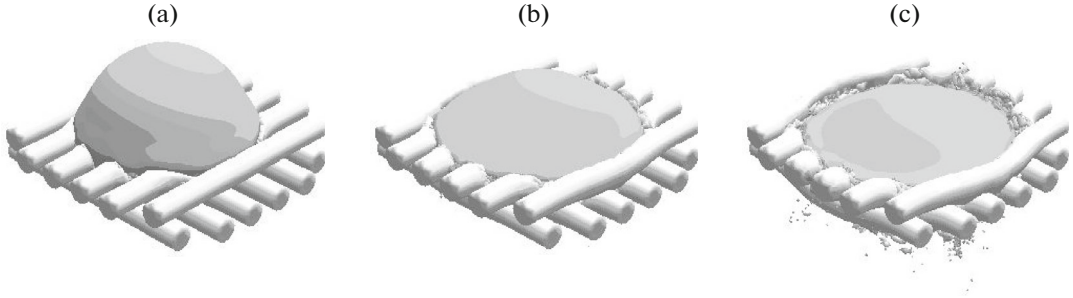

Fig. 1. Assembly of mesh and spherical particle in 3D view. Collision velocity of 3 km/s: (a) 0.3330 μs; (b) 0.5000 μs; (c) 0.6700 μs.

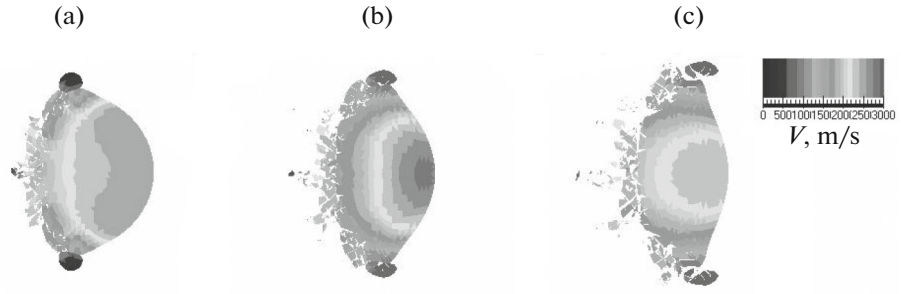

Fig. 2. Two-dimensional section of mesh and spherical particle. The distribution of velocity: (a) 0.3330 μs; (b) 0.5000 μs; (c) 0.6700 μs.

In the three-dimensional statement, the problem of penetrating a two-layer barrier (glass-fiber plastic ST-NT + D16 alloy) with a ball of steel SHKH-15 was considered. Calculations were performed on the collision of the ball and barrier along the normal to the surface of the latter. The velocity of the striker was equal to 700 and 900 m/s. The comparison of the numerical results with experimental data showed a quite satisfactory coincidence.

In the three-dimensional statement, the problem of the penetrating a two- and three-layer barrier (steel–ceramics, steel–ceramics–steel) by a cylindrical striker of tungsten alloy was considered. The comparison of the numerical results (n) and the experimental (e) data [14] showed a good agreement between the remaining lengths (l_n and l_e) and velocities (V_n and V_e) of the striker for the cases of two- and three-layer barriers. The two-layer barrier: $l_e = 37$ mm, $V_e = 1120$ m/s; $l_n = 35$ mm, $V_n = 1200$ m/s. Three-layer barrier: $l_e = 11.5$ mm, $V_e = 890$ m/s; $l_n = 10.0$ mm, $V_n = 855$ m/s.

4. NUMERICAL SIMULATION OF COLLISION OF HIGH-SPEED PARTICLES WITH MESH SHIELD SPACECRAFT ELEMENTS

1. The interaction of a striker with the first barrier mesh. As a shield, we consider two meshes placed before the spacecraft body. At the first stage of calculation, we consider the interaction of a spherical particle with a first shield mesh. The material is aluminum for the barrier and the ball, steel for the mesh, and the diameter of the thread is 0.32 mm for the first mesh and 0.2 mm for the second. The thickness of the barrier is 1.85 mm and the ball diameter is 2 mm. The distance between the meshes is 1 cm, and that between the barrier and the second mesh is 2 cm.

The calculation results of the interaction of a spherical particle with the mesh at the collision velocity of 3 km/s are shown in Figs. 1–2.

As particle velocity increases, the degree of fragmentation of the latter is significantly enhanced with the formation of a fragmentation cloud colliding with the second mesh.

2. The motion of fragments of the mesh and the striker from the first to the second mesh. Figure 3 shows two stages of particle interaction with shield meshes. The interaction of the first barrier with a high-speed particle is shown in Fig. 3a.

Here is noted the intense fragmentation of the particle and mesh with the formation of fragment flux moving toward the second barrier (Fig. 3b).

3. The interaction of the particle remainder with the spacecraft body. The main danger for the second barrier is the core of the fragment flux, which can be clearly seen in these figures and represents the nondestructive part of the high-speed particle. The picture of the interaction of this core with the second mesh is

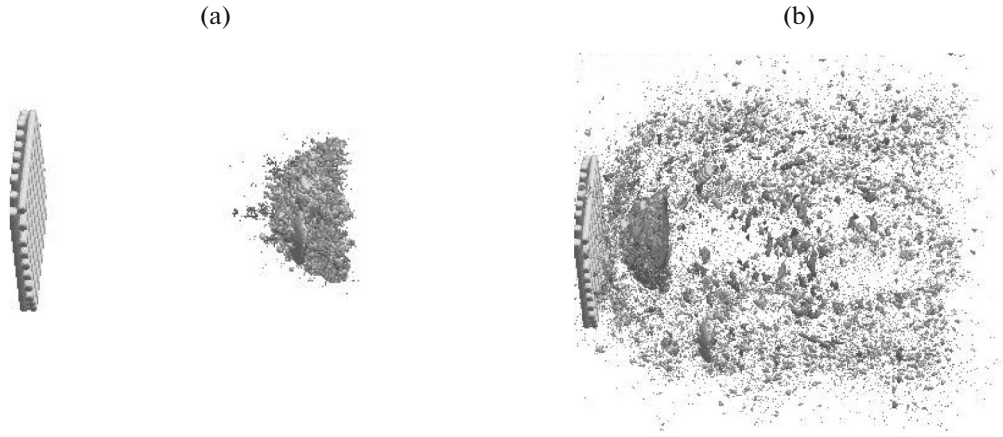

Fig. 3. Initial velocity of collision of a particle with first mesh–barrier of 3 km/s: (a) 0.8800 μs; (b) 5.5000 μs.

qualitatively similar to the picture of the particle interaction with the first mesh. The main interest is the interaction of the remainder of the particle with the spacecraft body in order to penetrate it or conserve the integrity of the latter.

The picture of the deceleration of the remainder of the basic particle in the spacecraft body for collision velocities of 3 km/s is shown in Fig. 4. The penetration of the body does not occur, which is also confirmed by the experimental data presented below.

5. ANALYSIS OF EXPERIMENTAL DATA ON THE INTERACTION OF A HIGH-SPEED PARTICLE WITH A SOLID SURFACE SIMILAR TO CRITICAL ELEMENTS OF SPACECRAFT DESIGN USING MESH DESIGNS AS PROTECTIVE SHIELDS

1. Experimental throwing facilities. For experimental studies of the processes of high-speed collision in a wide range of velocities (2–8 km/s) and masses of throwing elements, an experimental stand with a vacuum chamber and universal bed was developed and put into operation. The stand is equipped with the family of single-stage powder guns with calibers of 5.6, 8, 12.7, and 23 mm, as well as light-gas guns belonging to the PKH complex [19]. A gun with an 8-mm caliber produces a velocity of 2.2 km/s for assemblies with a mass of 1–2 g. For ultralight assemblies ($C_q \leqslant 1$ g/cm^3) and using combined powder charges, the velocity can be increased by 200–300 m/s.

Light-gas gun MPKH 23/8 is the simplest light-gas gun "with a heavy piston" and consists of three main details: a piston barrel, a ballistic barrel, and an electric fuse plug. Light-gas gun MPKH 23/8 is designed to obtain velocities up to 5 km/s for assemblies with $C_q = 1–3$ g/cm^3. The gun is very easy to service and can be operated with commonly used powders (VT) or hunting powders (Sokol, Bars, and others).

Light-gas gun PPKH 34/8 is a classic light-gas gun with a light piston and is designed to obtain velocities up to 8 km/s and higher for assemblies with $C_q = 1–3$ g/cm^3.

In the experiments carried out, it was necessary to separate a pan from a throwing element, which is sufficiently complex problem. A scheme was developed and implemented of the "power" separation of the pan and the striker. For this purpose, on the axis of the shot behind the muzzle velocity sensor, a multilayer barrier was installed with a hole exceeding the diameter of the striker by a factor of 1.5–2. We studied several versions for a multilayer barrier: (1) the base is plate of duralumin D16 with thickness of 30 mm, steel plate with thickness of 8 mm, rubber with thickness of 6 mm, and lead with thickness of 6 mm; (2) from the top, a steel plate with thickness of 6 mm is added. Experiments have shown that the second version is more appropriate. In this case, at velocities more than 2 km/s, it is necessary to increase the thickness of the upper plate up to 10 mm. The plate base is rigidly connected with the barrel by means of four supporting arms of steel angles, which, in turn, are strengthened to the two steel rings strengthened to the barrel. A multilayer barrier of steel–rubber–lead–steel has the abil-

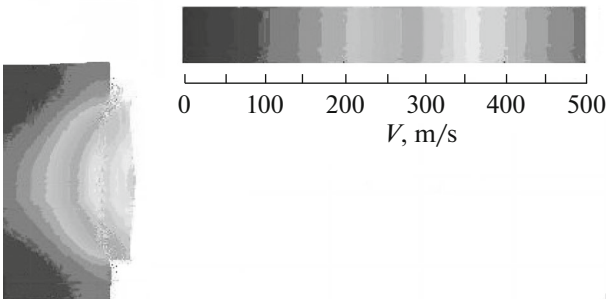

Fig. 4. Collision velocity of 3 km/s: distribution of velocity for particle and barrier at time instant $t = 25.9053$ μs.

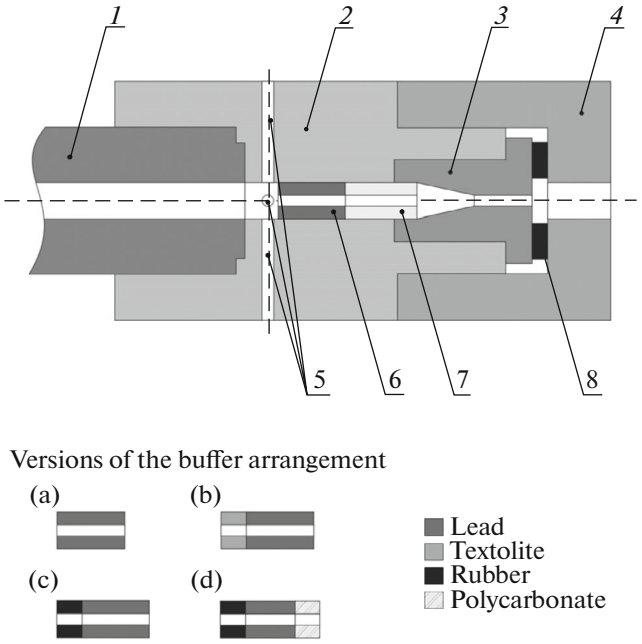

Fig. 5. Scheme of cutoff for SPbSU MPKH 23/8 with 8-mm caliber.

ity to move along the plate base with two micrometer screws for the precise alignment of the center of the hole with the axis of the shot. For the exact designation of the axis of the shot, a system of laser sighting was developed, including the input caliber with the system of mount and adjustment of the laser and the output caliber, mounted on a titanium tube to install it in the muzzle barrel cut through the muzzle velocity sensor. In the input and output calibers a central hole with a diameter of 1 mm was created. The laser is adjusted in such a way that the beam passes through the holes in the input and output calibers, which allows us to precisely combine the holes in the barrier with the axis of the shot. This scheme is considered in more detail in [17].

It should be noted that for the power cutoff method, the fragments of the pan and cutter penetrate into the hole and interact with the shield. However, in view of the fact that they have other lower velocities, holes punched in the shield differ from holes punched by a ball.

These defects are omitted for a ballistic facility with cutter [18], where a complete cutoff not only of elements (fragments) of the pan, but also of throwing gas is provided. The scheme of a cutter for LSU MPKH 23/8 with a caliber of 8 mm is shown in Fig. 5.

The cutter consists of a nozzle *2* of steel OKHNZMFA-090, which is mounted (screwed) to barrel *1*. In the nozzle, there is a seat for the insert *3* with the central cylinder-conic channel. The diameter of the input channel is equal to the caliber of the barrel of 8 mm, and the output hole is larger than the diameter of the throwing ball by a factor of 0.5–1 mm. The angle of the cone opening was taken equal to 10°–20°. The insert *3* is pressed to the nozzle *2* with the nut *4* through a rubber damper. Before the insert, the buffer *6* and the deformable cutoff *7* are mounted. Before the buffer *6* in the nozzle *2*, there are several holes *5* with a diameter of 6 mm for the depressurization of throwing gas behind the throwing assembly.

The facility with the cutter operates as follows. After accelerating the assembly (duralumin ball in a pan of the medium strength textolite), the latter strikes the buffer, the pan is decelerated and destroyed, but the ball flies through the hole in the buffer and the deformable cutter. The buffer *6* pushes the deformable cutter *7*, which enters into the conic channel of the insert, so that the channel in it collapses and cuts fragments of the pan and throwing gas.

During the experimental testing of the ballistic facility with cutter, as well as during experimental studies, various combinations of buffers and deformable cutters were tested. In this case, it was found that deformable cutters of PVD (high-pressure polyethylene) and SVMP (super high-molecular polyethylene), when collapsed, form a cumulative jet that distorts the picture of the collision. Therefore, other materials were used. Moreover, in this set of experiments together with the cutter, the sensor of muzzle velocity of the throwing assembly is not used. Therefore, before a concrete set of experiments, a control shot was carried out with the muzzle velocity sensor, and the set was continued with selected parameters of charging. As a result of this, a significant part of the tests was found to be either not tested or going beyond the requirement of the specifications for the mass of throwing element, although, in this case, the experiments give a representation on the action of space debris (diameter of about 8 mm and mass of 0.42–0.47 g). For the facility we used as systems a powder gun with caliber 5.6 mm (PP 5.6) and a light-gas gun with caliber 8 mm (MPKH 23/8), with a cutter and a muzzle velocity sensor.

2. Experimental data on the protective properties of the mesh barriers. The results of the experimental testing of the ballistic facility with cutter, as well as the results of interactions of different strikers with a plate of AMG6 with thickness of 1.85 mm (tank) with various types of protection are presented in the table.

Figure 6 shows the front side of the assembly of the two meshes–tank element. In the same place, some experimental numbers are given from the table.

Thus, as a result of the performed studies, experimental data were obtained to check the adequacy of the used mathematical models and numerical calculation methods. Moreover, comparison of tests F20 and F21, F23 and F24, and especially tests F26 and F27 shows that a shield of two meshes of 0.32 and 0.2 mm is more effective than a single-layer duralumin barrier with a thickness of 1 mm (equivalent to mass).

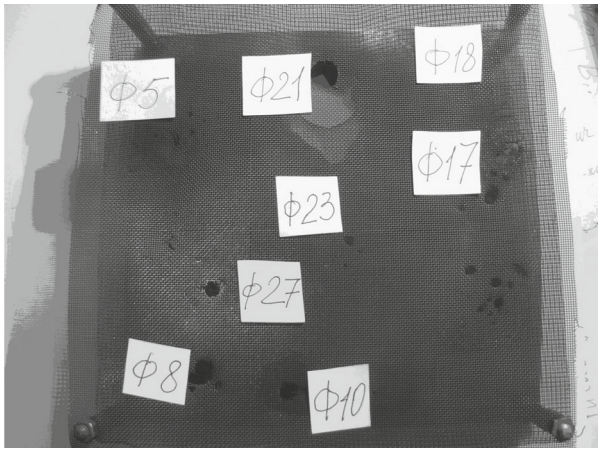

Fig. 6. Face of the assembly of two meshes–tank element.

CONCLUSION

We performed an analysis of experimental data of the interaction of a high-speed particle with a solid surface similar to critical elements of spacecraft design, using mesh designs as protective shields and having physical and technical properties of materials used in critical elements of the spacecraft design. The mathematical simulation of designs of protective shields providing acceptable resistance to the influence of meteorites for critical elements of the spacecraft design taking into account given limiting ballistic dependencies was implemented. Equations were derived that describe the motion of a compressible elastic-plastic body taking into account the probabilistic nature of destruction. We performed a numerical study of the interaction of high-speed particles with layered spaced barrier in the form of critical elements of the spacecraft design and mesh designs of protective shields. We proposed a physical and mathematical model of a probabilistic process of fragmentation of solids at impact interaction and a numerical method of the implementation of this model with the automatic generation of a tetrahedral mesh allowing one to calculate bodies of arbitrary geometry. The questions of simulating the destruction of solids, probabilistic destruction mechanism, simulating initial inhomogeneities were considered. We performed the test calculations of the fragmentation of thick-walled elastic-plastic cylindrical shells under explosive stressing with a 2D approach, a test 3D calculation using the probabilistic approach, a test calculation of penetrating a layered barrier along the normal and at an angle to the surface, and a test calculation of penetrating the protection shield along the normal to the surface. We presented the results of the numerical simulation of high-speed particle collisions with the mesh protection elements of the spacecraft, including the interaction of the striker with the first mesh barrier and considered the motion of fragments of mesh and striker from the first to the second mesh.

The method for solving the problems of fragmentation based on a probabilistic approach to the process of destruction of solids allowed us in the most complete, from a physical point of view, three-dimensional formulation to adequately reproduce the processes of the fragmentation of bodies under the action of explosive and shock loads. The numerical results confirmed the possibilities of the proposed probabilistic approach and numerical method to simulate the processes of natural fragmentation of design elements under intensive dynamic loading. Consequently, the researcher had the opportunity to influence the nature of fragmentation spectra of the considered design by varying the physical and mechanical parameters and the material structure. The results are a step in the study of the processes of collision of technogeneous and natural high-speed fragments with elements of spacecraft design.

ACKNOWLEDGMENTS

This work was supported by the Ministry of Education and Science of the Russian Federation in the framework of the state assignment no. 2014/223, project no. 1567.

REFERENCES

1. Whipple, F.L., Meteorites and space travel, *Astron. J.*, 1947, no. 1161, p. 131.
2. Shumikhin, T.A., Bezrukov, L.N., and Myagkov, N.N., A model experiment elucidating the mechanism of fragmentation of high-speed bumper on discrete screens, *Mekh. Kompoz. Mater. Konstr.*, 2007, vol. 13, no. 3, pp. 341–355.
3. Christiansen, E.L., Advanced meteoroid and debris shielding concepts, 1990, AIAA Paper 90-1336.
4. Christiansen, E.L. and Kerr, J.H., Mesh double-bumper shield. A low-weight alternative for spacecraft meteoroid and orbital debris protection, *Int. J. Impact Eng.*, 1993, vol. 14, nos. 1–4, pp. 169–180.
5. Horz, F., Cintala, M., See, T., et al., Comparison of continuous and discontinuous collisional bumpers: Dimensionally scaled impact experiments into single wire meshes, *NASA/TM*, 1992, no. 104749.
6. Shumikhin O., Semenov, A., Bezrukov, L., Malkin, A., Myagkov, N., and Kononenko, M., On fragmentation of aluminum projectile on mesh bumpers, *Proceedings of the Fourth European Conference on Space Debris, 18–20 April 2005*, Darmstadt, Germany: ESA/ESOC, 2005, p. 471.
7. Bezrukov, L.N., Shumikhin, T.A., and Myagkov, N.N., Ballistic properties of mesh protective constructions at high-speed bumping, *Mekh. Kompoz. Mater. Konstr.*, 2008, vol. 14, no. 2, pp. 202–216.
8. Wilkins, M.L., Calculation of elastic plastic flow, in *Methods in Computational Physics*, Alder, B., Ed., New York: Academic, 1964, pp. 211–263.
9. Wilkins, M.L., Modelling the behavior of materials, in *Proceedings of the International Conference on Structural Impact and Crashworthiness, 16–20 July 1984*, London: Elsevier Applied Science, 1984, vol. 2, pp. 243–277.

10. Bjork, R.L., Kreyenhagen, K.N., Piechocki, J.J., and Wagner, M.H., Ballistic limit determination in impacts on multimaterial laminated targets, *AIAA J.*, 1970, vol. 8, no. 12, pp. 2147–2151.

11. Johnson, G.R., Colby, D.D., and Vavrick, D.J., Tree-dimensional computer code for dynamic response of solids to intense impulsive loads, *Int. J. Numer. Methods Eng.*, 1979, vol. 14, no. 12, pp. 1865–1871.

12. Johnson, G.R., Dynamic analysis of explosive-metal interaction in three dimensions, *Trans. ASME, J. Appl. Mech.*, 1981, vol. 48, no. 1, pp. 30–34.

13. Glazyrin, V.P., Orlov, Yu.N., and Orlov, M.Yu., Modelirovanie razrusheniya materialov pri udare i vzryve, *Vestn. Akad. Voennykh Nauk*, 2008, no. 3, pp. 94–98.

14. *Teoreticheskie i eksperimental'nye issledovaniya vysokoskorostnogo vzaimodeistviya tel* (Theoretical and Experimental Studies on High-Speed Interaction of Bodies), Gerasimov, A.V., Ed., Tomsk: Tomsk. univ., 2007.

15. Diep, Q.B., Moxnes, J.F., and Nevstad, G., Fragmentation of projectiles and steel rings using 3D numerical simulations, in *Proceedings of the 21th International Symposium on Ballistics, 19–23 April 2004, Adelaide, Australia*, pp. 752–758.

16. Gerasimov, A.V. and Pashkov, S.V., Numerical simulation of penetration in layered targets, *Mekh. Kompoz. Mater. Konstr.*, 2013, vol. 19, no. 1, pp. 49–62.

17. Gerasimov, A.V., Pashkov, S.V., and Khristenko, Yu.F., Space vehicle protection from man-caused and natural debris—Experiment and numerical simulation, *Vestn. Tomsk. Gos. Univ.: Mat. Mekh.*, 2011, no. 4, pp. 70–78.

18. Gerasimov, A.V., Zharovtsev, V.V., and Khristenko, Yu.F., RF Patent no. 2400687, *Byull.*, 2010, no. 27.

19. Khristenko, Yu.F., The problem of obtaining high velocities of bumpers and models in laboratory conditions, in *Vserossiiskaya konferentsiya "Fundamental'nye i prikladnye problemy sovremennoi mekhaniki"* (All-Russian Conference "Fundamental and Applied Problems in Modern Mechanics"), Tomsk: Tomsk. gos. univ., 1998, pp. 211–212.

Translated by N. Topchiev